

SCIENTIFIC PAPERS
OF THE UNIVERSITY OF PARDUBICE
Series A
Faculty of Chemical Technology
23 (2017)

**CRYSTALLIZATION IN $Sb_{0.5}Se_{99.5}$ GLASS STUDIED
UNDER AND WITHOUT PROTECTIVE
ATMOSPHERE**

Pavla HONCOVÁ^{1a}, Petr PILNÝ^b, Stanislav STEHLÍK^a, and Petr KOŠŤÁL^a

^aDepartment of Inorganic Technology,

^bDepartment of Physical Chemistry

The University of Pardubice, CZ–532 10 Pardubice

Received May 4, 2017

The crystallization in a $Sb_{0.5}Se_{99.5}$ glass was studied by DSC method. The manipulation with amorphous samples was done under the protective atmosphere of argon and also without this protection, by simply exposing to the air. The obtained DSC traces as well as their kinetic characterization have shown that the atmosphere during the manipulation with amorphous material has significant influence on its crystallization behaviour.

Introduction

The chalcogenide materials are frequently studied for several decades because of their interesting optical and physical properties. Application, such as the data-

¹ To whom correspondence should be addressed.

recording devices and various opto-electronic elements require the amorphous state or utilize amorphous-to-crystalline changes in the chalcogenide material [1,2]. Thus, the knowledge of the crystallization process and of thermal stability is necessary before any production.

The Sb-Se glass is a binary system for which the crystallization behaviour has not been yet fully understood. However, our recent work [3,4] described that the discrepancy in the calorimetrically observable crystallization traces (one crystallization peak [5] or more complex behavior [6,7]) is a consequence of different particle sizes of the samples studied.

The aim of this work is to contribute to the description of crystallization behaviour of Sb-Se binary glass; particularly, to emphasize the effect of atmosphere (either inert or oxygen-containing air) used during the manipulation with amorphous sample on the crystallization behaviour observed by calorimetry.

Kinetic Analysis

The crystallization behaviour can be observed directly by microscopy or indirectly – frequently using the differential scanning calorimetry (DSC). The output signal of DSC is a heat flow, Φ , dependent on time (isothermal conditions) or temperature (non-isothermal conditions). The kinetic equation of DSC trace can be described as [8]

$$\Phi = \Delta H A e^{-\frac{E}{RT}} f(\alpha) \quad (1)$$

where ΔH is the enthalpy change of the process, A the pre-exponential factor, E the activation energy of the process, R the universal gas constant, T the temperature, $f(\alpha)$ the kinetic model and, finally, α the conversion. The procedure of kinetic analysis of single peak is described in many papers and books [8], where the determination of the activation energy is followed by selection of the appropriate kinetic model and determination of the respective parameters. The selection of kinetic model can be done either by parallel testing of several models, or a method of the characteristic function is being applied [9,10] or a typical shape of the peak (its symmetry) can signalize the optimal model [11]. In the case of overlapping peaks, their deconvolution is necessary for application of full kinetic analysis. The best approach for the deconvolution process is a simple numerical fitting with the aid of general equation that describes various shapes of the DSC peaks, such as the Fraser-Suzuki function [12-14] or a deconvolution based on selected function [15]. When the deconvolution of complex peak is finished; then, kinetic analyses of the single peaks obtained follow the same procedure as that for the simple process described above. The kinetic analysis of such a simple process, as well as the overlapping peaks can be done using free-available software OriTas

[16], where the standard kinetic equations are used for calculations.

The activation energy is frequently determined by the Kissinger method [17] evaluating the shift of temperature that corresponds to the maximum of crystallization peak, T_p , with the heating rate, β , where the slope of the $\ln(\beta/T_p^2)$ to $1/T_p$ dependence is equal to the $-E/R$ ratio. In the case of chalcogenide material, the crystallization is usually defined by the nucleation-growth model formulated by Johnson and Mehl [18] plus Avrami [19] (referred to as JMA) giving the following expression

$$f(\alpha) = n(1 - \alpha)[- \ln(1 - \alpha)]^{1 - \frac{1}{n}} \quad (2)$$

where the value of kinetic exponent n depends on the crystal growth morphology. Thus, the knowledge of the value of parameter n can lead to the proper interpretation of mechanism of the process studied. The mechanism of crystallization can be also confirmed by direct observation using a suitable microscopic technique; obviously, the best being the combination of both [4,20].

Experimental

The amorphous $\text{Sb}_{0.5}\text{Se}_{99.5}$ glass was prepared from pure elements by conventional melt-quenching method: the elements had been weighted into a quartz ampoule that was then evacuated, tightly sealed and put into the rocking furnace where the melting and homogenization were performed at temperature of 800 °C for 20 h and, consequently, at 600 °C for 4 hours; then the ampoule was quenched in a cold brine. When the total amount of the weighted elements was only 4 g and a thin layer of the melt in the ampoule was formed during cooling, then the prepared material became distinctly amorphous (otherwise, partially crystalline material was obtained). The amorphous nature of the samples prepared was confirmed by X-ray analysis, as well as by scanning electron microscopy (SEM) with the aid of optical and infrared microscopies. The samples after the crystallization were also examined by X-ray analysis and only the hexagonal selenium could be detected. Two batches of samples were prepared in order to test the effect of the atmosphere on crystallization. The samples for DSC analysis were prepared under protective atmosphere as well as without. The protective atmosphere of argon means that the manipulation, i.e. from the breaking of the ampoule to the closing of the sample into hermetically sealed aluminium pan for DSC analysis, was done in a protective glove-box filled with argon. Otherwise, the sample without protective atmosphere was exposed to ambient air (for common manipulation in the laboratory, i.e. oxygen-containing atmosphere). In all cases, the amorphous samples were in the bulk form as thin plates without any surface treatment and with similar mass about 10 mg.

The crystallization was studied using a Pyris 1 differential scanning calorimeter with intracooler 2P (Perkin-Elmer). The melting temperatures of several pure metals (namely: Hg, Ga, In, Sn, Pb, and Zn) were used to calibrate the temperature. The enthalpy was calibrated using a known enthalpy of fusion for In. The metals requiring calibration were weighted into aluminium pans that were also used for other experiments; the empty pan was used as a reference. The amount of calibration metals was 10 mg, the heating rate of 10 K min⁻¹ and the protective atmosphere of dry nitrogen with the flow rate of 20 ml min⁻¹.

The isothermal measurements of the samples were done in the temperature range from 95 °C up to 117 °C for a time period necessary to finish the crystallization process. The heating step came before isotherm when the sample was heated from 20 °C to temperature of isotherm by a rate of 150 K min⁻¹. The non-isothermal measurements were done in the temperature range from 20 to 215 °C at a heating gradient of 1, 2, 3, 5, 10, and 15 K min⁻¹. The illustration of crystallization traces that have been obtained in this way is given in Fig. 1 for both types of samples prepared under and without the protective atmosphere.

Results and Discussion

The kinetic study of amorphous Sb_{0.5}Se_{99.5} glass was done under the isothermal and non-isothermal conditions and the manipulation with the bulk samples was either under or without the protective atmosphere. Selected DSC traces for given heating rates or temperatures in Fig. 1 clearly show that the manipulation with the amorphous sample in the air (i.e. without the protective atmosphere of argon) accelerates the crystallization process — not only that the crystallization starts earlier but also the peak maximum proceeds at a shorter time compared to that for sample treated under the atmosphere of argon. Moreover, the shape of the main part of traces for sample without protective atmosphere is much broader in comparison with traces for sample treated under the atmosphere of argon.

However, the shape of DSC traces obtained both under isothermal and non-isothermal conditions evidently reflect the complex character of the crystallization process. The complex character of crystallization in the Sb-Se glass is not surprising because the crystallization of the pure selenium itself proceeds as complex process taking place at the surface and in the bulk when even two kinds of spherulites have been observed [20]. By taking this into account, the overlapped peaks in Fig. 1 involve crystallization of Sb₂Se₃ and the surface and bulk crystallization of selenium. Nevertheless, the amount of antimony in selenium is very low and no Sb₂Se₃ crystals have been detected by X-ray diffraction and also there is no evidence of its crystallization on the DSC traces. Therefore, the formation of crystals with Sb is neglected in further analyses of experimental data. Notwithstanding the addition of antimony into the selenium is only 0.5 %, the

result is that the main part of DSC traces cannot be described by the nucleation-growth model. As already described for isothermal crystallization of the bulk sample prepared under the protective atmosphere (see Ref. [4]) when the respective study for the argon atmosphere is depicted in Fig. 1B, the addition of antimony significantly influences the nucleation of selenium in the volume of the sample resulting in a time-lag that markedly grows with the decreasing temperature of annealing. The same behavior can then be expected for isothermal crystallization of samples prepared without protective atmosphere and additionally pronounced by the effect of air (oxygen). And also, the non-isothermal experiments should reflect this crystallization scheme as discussed later.

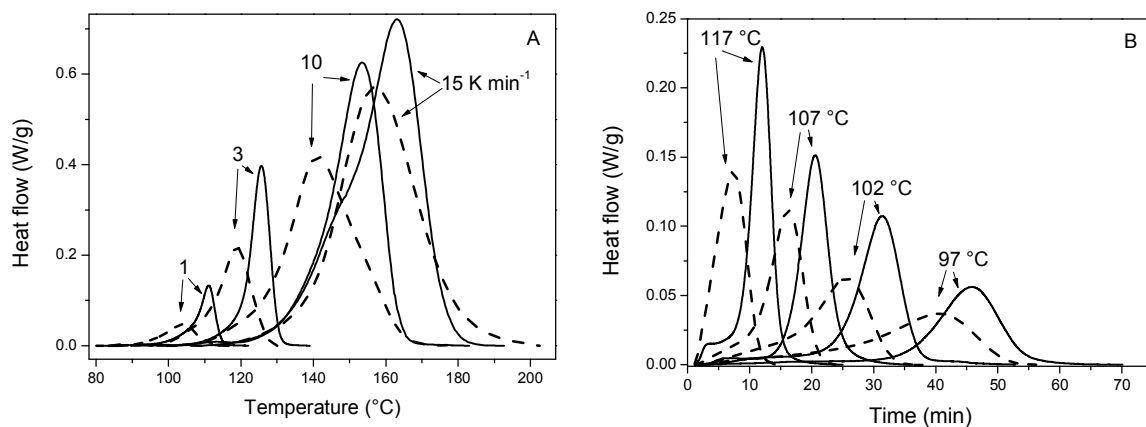


Fig. 1 The DSC traces of crystallization in $\text{Sb}_{0.5}\text{Se}_{99.5}$ glass under A) non-isothermal and B) isothermal conditions. The full lines correspond to the sample prepared under protective atmosphere and the dash lines to sample without protective atmosphere. The numbers correspond to A) heating rate or B) annealing temperature, respectively

The overall enthalpy change measured during the crystallization process has been found a bit lower for isothermal conditions compared to non-isothermal treatment and slightly higher for the sample prepared under protective atmosphere in confrontation with the samples without protective atmosphere. The exact values of ΔH are given in Table I. The difference between the ΔH values for isothermal and non-isothermal data was also observed for other chalcogenide materials [21,22]. It could be explained by a small heat loss in isothermal experiment due to a partial crystallization already started during the heating of the sample (although the rate was as high as 150 K min^{-1}) before attaining the annealing temperature. The difference between the overall ΔH values for samples prepared under and without protective atmosphere has been caused by the presence of oxygen. On one side, the presence of oxygen accelerates and facilitates the crystallization so that the heat released can be lower. On the other side, the accelerated crystallization reflects a more compact DSC trace (see Fig. 1), leading to a lower value of ΔH , when the enthalpy change can be calculated from the area

below the DSC trace.

The kinetic analysis by means of deconvolution was done using an OriTas software [16] and utilizing conventional kinetic models. The calculations were based on standard kinetic equations introduced above (in the section Kinetic Analysis). In the case of non-isothermal data, the value of activation energy can be determined by the Kissinger method [17] and the respective value is 63 kJ mol⁻¹ for the sample prepared under the protective atmosphere and 70 kJ mol⁻¹ for sample without the protective atmosphere. These values of activation energy were used for further kinetic analysis of the DSC data obtained under non-isothermal, as well as under isothermal conditions.

Table I The value of the enthalpy change ΔH obtained from the overall crystallization traces and the activation energy determined by Kissinger method

Atmosphere during the manipulation	Isothermal conditions	Non-isothermal conditions	
	$\Delta H, \text{J g}^{-1}$	$\Delta H, \text{J g}^{-1}$	$E, \text{kJ kmol}^{-1}$
Ar	-49 ± 8	-60 ± 4	63 ± 3
Air	-47 ± 2	-54 ± 5	70 ± 4

The deconvolution of DSC data started with assumption that the overall trace could be calculated as a sum of two crystallization peaks when utilising the value of E given in Table I. Thus, the best result was the closest fit to the overall DSC trace. The models used for data description were the JMA (defined by Eqn. 2) with parameter n and surprisingly obeying the Gaussian curve with three specific parameters

$$f(x) = Y e^{-\frac{(x-X)^2}{2w^2}} \quad (3)$$

where Y is the height of the curve's peak, X the position of the centre of the peak and w the width of the bell. The approximation by the Gaussian curve for the main part of crystallization trace demonstrates that the standard kinetic model cannot describe the time-lag already described in Ref. [4] for isothermal data of samples prepared under the protective atmosphere. Although the new nucleation-growth rate model involving the time-lag was suggested [4], it is valid up until now only for isothermal data and its application to non-isothermal data is a task for the future. That is why the standard JMA model and the Gaussian curve are used in this work to describe both isothermal and non-isothermal data.

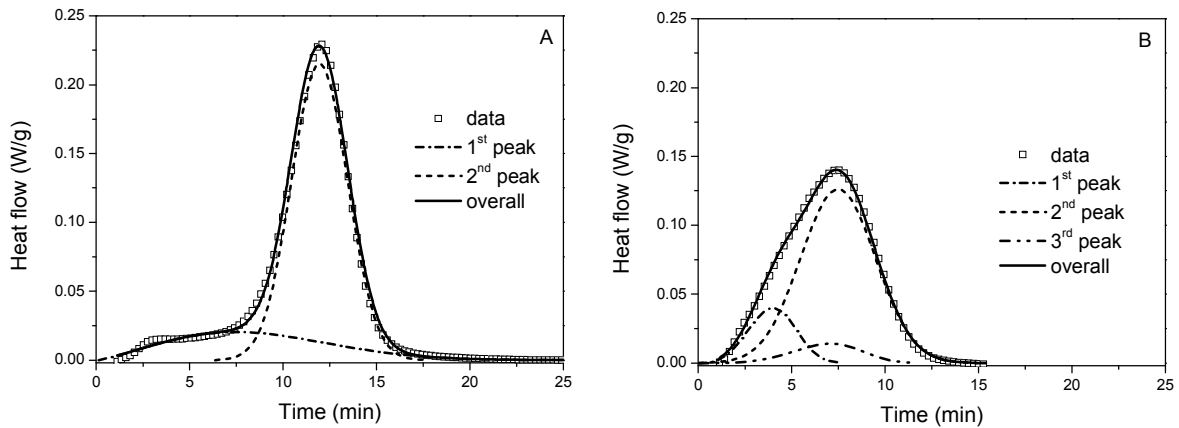


Fig. 2 DSC data obtained for crystallization at temperature of 117 °C and the sample prepared A) under and B) without the protective atmosphere. The deconvoluted peaks are illustrated together with the overall fitted curve

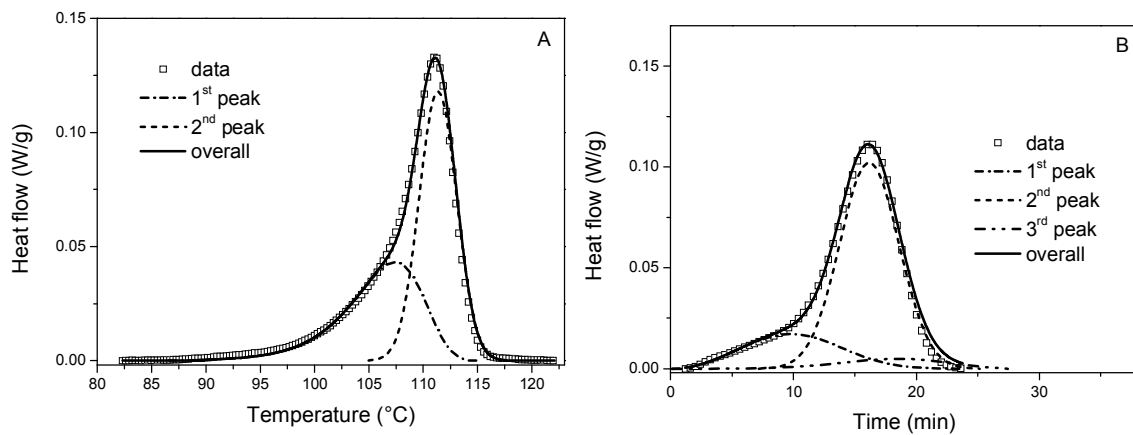


Fig. 3 DSC data obtained for crystallization at temperature of 107 °C and the sample prepared A) under and B) without the protective atmosphere. The deconvoluted peaks are illustrated together with the overall fitted curve

The deconvolution of isothermal data is illustrated in Figs. 2 and 3 for the sample prepared under and without the protective atmosphere. These results emphasize again the significant difference in the shape of DSC traces caused by the presence (air) or absence (argon) of oxygen during the preparation of the sample in crystallization experiments. This significant difference in the shape of DSC curve is subsequently reflected in the kinetic characterization. The overall crystallization trace obtained for the sample prepared under the protective atmosphere can be calculated as a sum of two peaks — the first small one corresponding to the crystallization of the selenium on the sample's surface, and the second main peak corresponding to the crystallization of selenium in the sample bulk together with the continuing growth on the sample's surface. (This explanation is in accordance with direct observation of crystal grow described in Ref. [4].) The first effect can be explained by the JMA model because there is no

time-lag, but the main effect must obey the Gaussian curve shape reflecting the shift of the beginning of the peak due to the time-lag. The corresponding parameters for both effects are summarized in Tables II and III.

Table II The values of the enthalpy change ΔH , the activation energy E , pre-exponential factor A , and parameter n of JMA model defining the first deconvoluted peaks for isothermal and non-isothermal conditions and the sample prepared under and without (air) the protective atmosphere. The set of parameters describing the third deconvoluted peaks for the sample prepared without protective atmosphere are given as well.

Conditions	Peak	$\Delta H, \text{J g}^{-1}$	$E, \text{kJ kmol}^{-1}$	$\ln (A/s)$	n	
Iso	Ar	1 st	-10 ± 2	65	13.5 ± 0.2	2.5 ± 0.2
	Air	1 st	-10 ± 3	70	15.7 ± 0.3	3.0 ± 0.4
		3 rd	-4 ± 1	70	15.3 ± 0.2	4.5 ± 0.4
Non-iso	Ar	1 st	-17 ± 3	63	13.4 ± 0.2	4.5 ± 0.8
	Air	1 st	-5 ± 2	70	16.4 ± 0.3	4.0 ± 0.8
		3 rd	-16 ± 4	56	10.9 ± 0.2	3.5 ± 1.0

Table III The values of the enthalpy change ΔH and the parameters of Gaussian function describing the second deconvoluted peaks for isothermal and non-isothermal conditions and the sample prepared under and without (air) the protective atmosphere. Gaussian function: a position of the centre of the peak X (in seconds for isothermal conditions and in Kelvins for non-isothermal conditions), height of the curve's peak Y and width of the bell denoted as w

Conditions		$\Delta H, \text{J g}^{-1}$	$X, \text{s; K}$	$Y, \text{W g}^{-1}$	w
Iso	Ar	-41 ± 6	$1\ 606 \pm 677$	0.13 ± 0.05	161 ± 56
	Air	-34 ± 5	$1\ 144 \pm 774$	0.10 ± 0.06	179 ± 87
Non-iso	Ar	-43 ± 7	408 ± 18	0.43 ± 0.21	3.6 ± 1.9
	Air	-35 ± 3	400 ± 16	0.24 ± 0.14	5.1 ± 1.9

On the contrary, the overall crystallization trace obtained for the sample prepared without protective atmosphere can be calculated as a sum of three peaks — the first and the second ones should have the same interpretation as in the case of the sample prepared under protective atmosphere, whereas the third peak reflects the presence of oxygen *via* some transformation of Se or Sb_2Se_3 involving oxygen. (This was similar to an observation described in Ref. [21] for crystallization of Sb_2S_3 , where the broadening of the decreasing part of DSC trace can be associated with transformation of Sb_2S_3 into SbO_2) The first and the third effect are described by the JMA model with the parameters summarized in Table

II, whereas the main effect is fitted by Gaussian curve with parameters given in Table III. As seen, the enthalpy change during the third effect is quite low compared to other two effects and this effect is described by the JMA model with rather high value of parameter n . Its high value enables to shift the peak position below the main effect or almost to the end of the overall curve (see Figs 2 and 3).

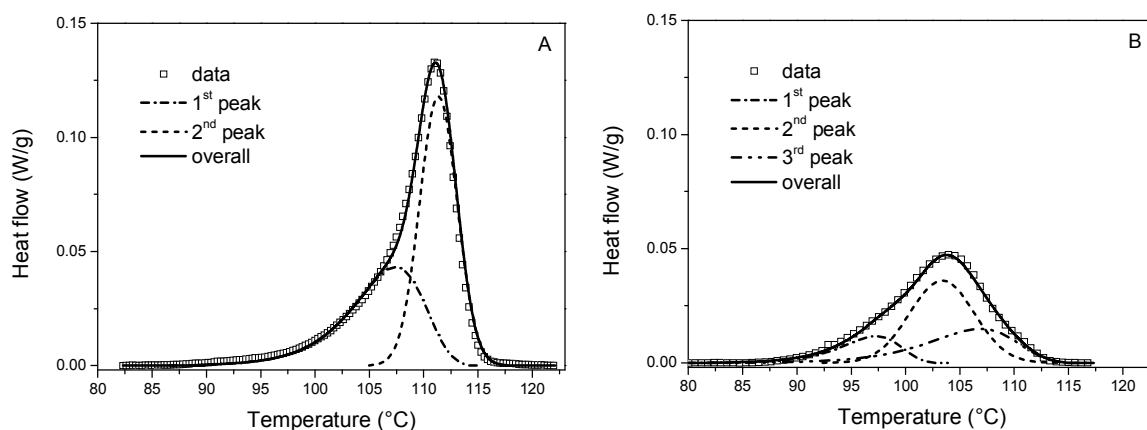


Fig. 4 DSC data obtained for non-isothermal crystallization at heating rate of 1 K min^{-1} and the sample prepared A) under and B) without the protective atmosphere. The deconvoluted peaks are illustrated together with the overall fitted curve

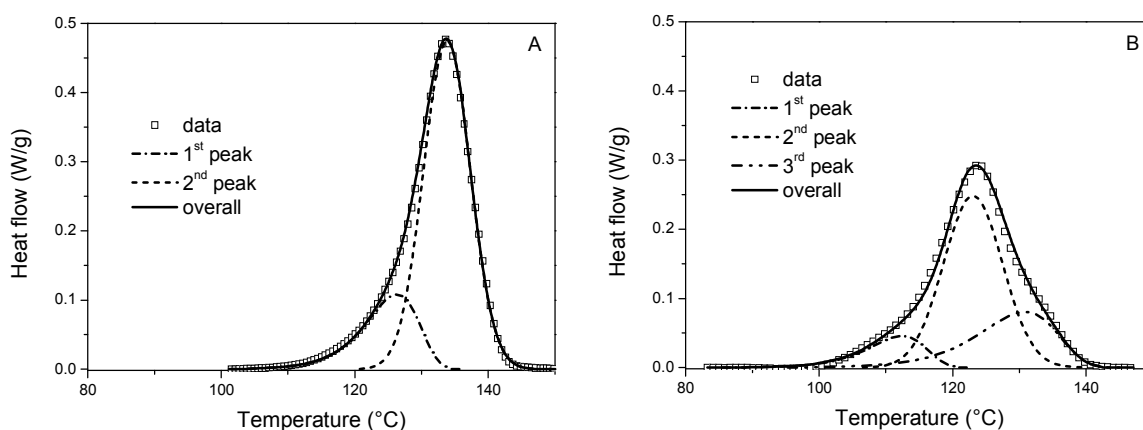


Fig. 5 DSC data obtained for non-isothermal crystallization at heating rate of 5 K min^{-1} and the sample prepared A) under and B) without the protective atmosphere. The deconvoluted peaks are illustrated together with the overall fitted curve

Similar results were obtained by deconvolution of non-isothermal data (see Figs 4 and 5 and parameters in Tables II and III). The only difference was the position and area of the third peak for sample prepared without the protective atmosphere. The area of the third signal is almost a half of the main-peak area caused by the shoulder on the decreasing part of the overall DSC traces (see Figs 1A, 4 and 5). One again, the third peak should be related with the transformation involving oxygen in a way as for the isothermal measurement and sample prepared

without the protective atmosphere. The value of parameter n of the JMA model describing the third peak was slightly lower in comparison with the isothermal data and also the value of activation energy being lower compare to the first peak.

Conclusion

The differential scanning calorimetry has been used to study the crystallization in $\text{Sb}_{0.5}\text{Se}_{99.5}$ glass under isothermal and non-isothermal conditions. The manipulation with bulk sample from the glass preparation up to its closing into a crucible for DSC measurement was done under the protective atmosphere of argon or without the protective atmosphere (i.e., in the air). As found out, this change in the atmosphere surrounding the glassy material significantly influences the shape of crystallization of the DSC traces and, subsequently, their kinetic behaviour. Even if the addition of antimony into selenium is low it has caused the time-lag of crystallization in the bulk of the sample leading to a kinetic model of the Gaussian curve type.

References

- [1] Hewak D.W.: *Chalcogenide Glasses for Photonic Device Applications. In Photonic Glasses and Glass-ceramics*, Research Signpost, 2010.
- [2] Adam J.L., Zhang X.: *Chalcogenide Glasses: Preparation, Properties and Applications*, Elsevier, 2014.
- [3] Honcová P., Pilný P., Svoboda R., Shánělová J., Košťál P., Barták J., Málek J.: *J. Therm. Anal. Cal.* **116**, 613 (2014).
- [4] Honcová P., Shánělová J., Barták J., Málek J., Košťál P., Stehlík S.: *Cryst. Growth Des.* **16**, 2904 (2016).
- [5] Holubová J., Černošek Z., Černošková E.: *J. Optoelectron. Adv. Mater.* **1**, 663 (2007).
- [6] Mehta N., Tiwari R.S., Kumar A.: *Mater. Res. Bull.* **41**, 1664 (2006).
- [7] El-Zaidia M.M., El-Shafi A., Ammar A.A., Abo-Ghazala M.: *Thermochim. Acta* **116**, 35 (1987).
- [8] Šesták J.: *Thermophysical Properties of Solids, Their Measurement and Theoretical Analysis*, Elsevier, 1984.
- [9] Málek J.: *Thermochim. Acta* **355**, 239 (2000).
- [10] Málek J.: *Thermochim. Acta* **200**, 257 (1992).
- [11] Málek J., Criado J.M.: *Thermochim. Acta* **164**, 199 (1990).
- [12] Fraser R.D.B., Suzuki E.: *Anal. Chem.* **41**, 37 (1969).
- [13] Perejón A., Sánchez-Jiménez P.E., Criado J.M., Pérez-Maqueda L.A.: *J. Phys. Chem. B* **115**, 1780 (2011).

- [14] Svoboda R., Málek J.: *J. Therm. Anal. Cal.* **111**, 1045 (2013).
- [15] Moharram A.H., Abu El-Oyoun M., Rashad M.: *Thermochim. Acta* **555**, 57 (2013).
- [16] Pilný P.: OriTas Program – A Solution for Kinetic Analysis of Thermoanalytical Data, <http://www.petrpilny.cz/oritasen>.
- [17] Kissinger H.E.: *Anal. Chem.* **29**, 1702 (1957).
- [18] Johnson W.A., Mehl K.F.: *Trans. Am. Inst. Min. Metall. Eng.* **135**, 416 (1932).
- [19] Avrami M.: *J. Chem. Phys.* **7**, 1103 (1939).
- [20] Málek J., Barták J., Shánělová J.: *Cryst. Growth Des.* **16**, 5811 (2016).
- [21] Pustková P., Zmrhalová Z., Málek J.: *Thermochim. Acta* **466**, 13 (2007).
- [22] Svoboda R., Málek J.: *J. Therm. Anal. Cal.* **119**, 1363 (2015).